2011 International Conference on Environmental and Computer Science
IPCBEE vol.19(2011) © (2011) IACSIT Press, Singapore

Automatic Road Extraction on Aerial Photo and Laser Scanner Data

Claudionor Ribeiro da Silva [1 +], Jorge Antônio Silva Centeno [2] and Maria João Henriques [3]

[1] Federal University of Uberlândia (UFU), Campus Monte Carmelo / MG, Brazil
[2] Federal University of Paraná (UFPR), Department of Geomatics, Curitiba/PR, Brazil
[3] National Laboratory for Civil Engineering (NLCE), Lisbon, Portugal

Abstract. Digitizing road maps manually is an expensive and time-consuming task. In this work we introduce a method, based on the iterative and localized Radon transform and optimal algorithms, which extracts automatically roads on images and airborne laser scanners of rural areas. The proposed method detects linear segments iteratively and starting from this it generates the roads centerlines. The results of the tests were presented and discussed, and the quality of the detected roads centerlines was computed. The values obtained reveal that the proposed method can be promising.

Keywords: Radon Transform; Laser scanner; Road extraction

1. Introduction

The availability of road databases is a necessity for the development of a village, a city and/or a municipality. In developing countries there are usually a large number of roads in the rural areas. For example, Brazil has about of 1725000 km of roads, being 90% of these in rural areas.

The need of high quality road maps is increasing, accordingly to the growing number and complexity of new and more robust software that demand such spatial information. However, vectorization and manual generation of road maps are expensive and time consuming processes.

Several approaches have been developed with the main purpose of automating or at least semi-automate that process. The aim of this work is the extraction on digital images and laser scanner data of roads in rural areas using the Radon transform and optimal algorithms.

A detailed description of the proposed method is presented in the next sections.

2. Road Extraction

The extraction of roads and other ways on digital images is a subject quite researched. There is a variety of techniques that can be found in the extensive bibliography that has been published on this matter. As examples, works that make use of aerial photographs can be seen at [1], [9] and [11]. Ikonos and QuickBird images were used at [11]. In [2] and [10] have been proposed techniques of road extraction using Spot images. The methods of road extraction using digital images are also classified according to image resolution: on low-resolution images [7] and on high-resolution images ([6], [9] and [11]).

Recently, altimetrics data was also introduced as information source ([3], [12] and [13]). The use of altimetrics data, alone or together with digital images, is still an emerging theme, that deserves further research.

[+] Corresponding author. Tel.: +55 (34) 3842-8751; fax: +55 (34) 3842-8748.
E-mail address: crs@ig.ufu.br .

The differences among techniques of road extraction are closely related to the used strategy. As examples, the use of Fuzzy Logic [2], Artificial Neural Networks [15], Genetic Algorithms [8], Radon Transform ([5], [11] and [15]) and the application of local and/or global strategies [9].

Several methods applied in road extraction depend on the detection of edges and/or lines. There is the detection of edges on digital images, like the algorithms of Canny, Prewitt and Sobel ([14]). The methods that depend on the detection of lines are presented by [14].

The approaches used in road extraction are based in intrinsic characteristics related to that feature. These characteristics are: radiometric, geometric, topological, functional and contextual. Therefore, the road model takes into account those characteristics.

3. Data end Method

The used dataset is composed by aerial photos and Laser scanner data obtained on a rural region from Paraná State (Brazil). In order to reduce the computational effort, it was only used the Red band of the photo. The Red band was smoothed and resampled to the same spatial resolution of the Laser scanner data (0.8 meters), and later was georeferenced in order to be used jointly with the Laser scanner data. There were also used the software package Multispec W32, to manipulate the images, and the platform MatLab, to develop the subroutines.

3.1. Cross-section and Road Width

The proposed method to extract roads in rural areas is composed by the detection of segments seeds and sequential detection of consecutive lineal segments. The process of detection of segments is accomplished through cross-sections of the roads.

A cross-section is represented by a set of digital values that compose a line that is straight or curved and is transversal to the road. The cross-section is constructed on the basis on road width (w). This cross-section presents the following characteristics: a) is one-dimensional and can be stored in a vector; and b) its size is greater that the width (w) of the studied road.

The road width (w) is measured by the method proposed in [4]. It is defined in function of the measured gradients in the margins of the road. The average distance among the two gradients is used as the road width.

3.2. Detection of Seed Segment

The proposed method of detection of segments uses the Radon transform. According to [11], the Radon transform, in continuous terms, is the projection of function $f(x, y)$ by function $TR(x', \theta)$, where $(x, y) \in R^2$, $x \in R$ and $\theta \in [0, \pi)$. The mathematical model of the Radon transform (TR) is presented in (1).

$$TR(x', \theta) = \iint f(x, y) * \delta(x * \cos\theta + y * \sin\theta - x')\, dxdy \qquad (1)$$

where θ is the direction of the vector orthogonal to the line under study; and δ is the Dirac function, that has the value zero everywhere except at x = 0 where its value is infinitely large in such a way that its total integral is 1.

Fig. 1 show an example of application of the Radon transform, where the dark point in the image corresponds to the existence of a straight segment.

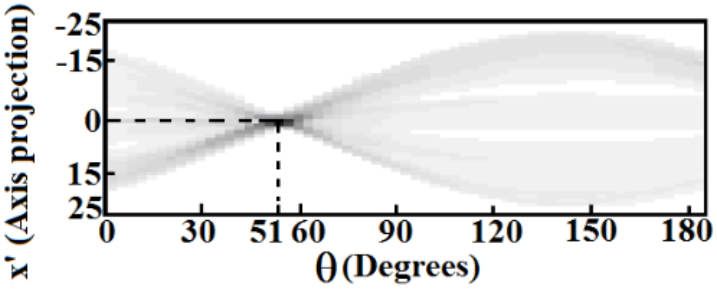

Fig. 1: Result of the Radon transform.

To facilitate the application of Radon transform, the original image is subdivided in sub-images, as show a Fig. 2.

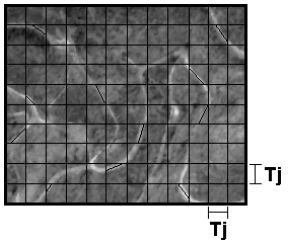

Fig. 2: Image subdivided with possible segments seed.

In each sub-image it is extracted a segment that later is analyzed by an objective function (2), evaluating your correlation with road centerline. If the analyzed segment presents correlation larger than a certain threshold T it is selected to be seed segment, otherwise, it is discarded.

$$FO = a * pC + b * pS \quad (2)$$

where a and b are the weights and $b = 1 - a$; pC is the correlation among two cross-section (reference $\vec{vr}$ and analyzed in the image $\vec{vs}$) of road; it is defined by the coefficient of correlation of Pearson (r), measured among the digital values of two referred cross-sections; and pS is the similarity among two cross-section of road.

The parameter related with the correlation between cross-sections is measured using (3).

$$pC = \begin{cases} r & \text{if} \quad r \geq 0 \\ 0 & \text{if} \quad r < 0 \end{cases} \quad (3)$$

The rural roads are built of exposed soil; therefore they present high reflectance in the red band. Due to this fact, the maximum digital value (vm) of the image is used in the measure of the similarity (4).

$$pS = e^{\left(\frac{-Dm(vm,vs)}{1000}\right)} \quad (4)$$

where e is the exponential function; Dm is the distance of Mahallanobis between the value vm and all the pixels of the cross-section $\vec{vs}$, measured during each iteration.

3.3. Searching for New Segments

The searching process for the best linear segment is successive and iterative. In Fig. 3 the grey thick line represents the road that is to be detected. In this phase the first section (segment 1-2) was already detected. The new segment (segment 2-Pi) and the previous segment (segment 1-2) are consecutive. The new segment is defined by the parameters λ and R, where λ is the angle that the previous segment makes with the x-axis, measured anticlockwise, and R é is the radius of the circular arch.

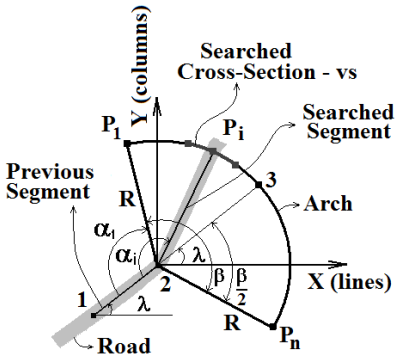

Fig. 3: Parameters used to detect the new segment.

A search region is defined using the point 2, the direction λ, and the angle β, that is defined by the user.

The best cross-section ($\vec{vs}$) is investigated in all the n possible positions (P_i) of the arch and is evaluated and weighed through of objective function (FO). A new parameter related with the previous segment is inserted in the function FO. That is possible because in this phase the previous segment (seed) is already known.

The search direction of the new segment is computed on the basis on angle α_i defined between the two vectors: previous and the new segment (see Fig. 3). Therefore, a new parameter (pD) is defined in (5).

$$pD = \begin{cases} |\cos(\alpha_i)| & \text{if} \quad \pi - \frac{\beta}{2} \le \alpha_i \le \pi + \frac{\beta}{2} \\ 0 & \text{otherwise} \end{cases} \qquad (5)$$

The integration with Laser scanner data is defined with the insert of a fourth parameter (pL) to the function FO. The parameter pL is defined by (6).

$$pL = e^{(-RMS)} \qquad (6)$$

where RMS (root mean square) is processed using the distances dt_i measured from all the altimetrics points until the rectangular plane under analysis. The distance from a point $P(x_1,y_1,z_1)$ to a plane is determined by normal vector N(A,B,C) and point $Q(x_0,y_0,z_0)$, where A, B e C are the coefficients of the equation of the plane.

The new objective function is defined by (7).

$$FO = a * pC + b * pD + c * pS + f * pL \qquad (7)$$

where a, b, c and f are the weights, with $f = 1 - (a + b + c)$.

4. Preliminary Experiments

The parameters R and β and the coefficients of the equation FO are empirically defined. In the experiments R = 17 pixels; $\beta = 90^0$ and the coefficients (weights) they varied in the interval [0 1].

For comparison, two experiments had been carried out. The first one uses only the digital image, and the second one uses the same digital image integrated with Laser scanner data. The results are illustrated in Figs. 4 and 5, respectively.

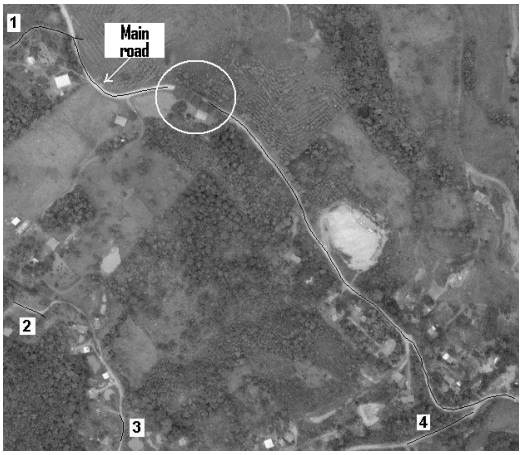

Fig. 4: Results using only the digital image.

Fig. 5: Results using digital image and Laser scanner data.

Considering only the main road centerline is noticed visually that the completeness is superior when the integrated data is used. Especially in the place where happens obstruction of the lane with shades of trees

(circumference in Fig. 4). In the narrow roads centerlines detection (points 1, 2, 3 e 4 in Fig. 4) the Laser scanner data do not contribute, because in narrow roads the width alters abruptly, and the points altimetrics that do not belong to the road lane are analyzed in the rectangular plane (w x R) as belonging to these roads. The erroneous insert of those points cause errors in the detection process.

The results obtained in [12] present accuracy 1.70, 0.84 and 0.80 in terms of RMS, completeness and correctness, respectively. In the proposed method the same accuracy measures showed values of 1.59, 0.85 and 0.80, respectively. It is noticed that the results are similar; however, although preliminary, the proposed method had advantages in terms of geometric quality (11%).

5. Final Considerations

The total obstruction of the lane road (e. g. shadow of trees) is a serious problem in the process of road detection, using only digital image; the Laser scanner data is useful information to solve this problem. The result of the experiments shows the possible contribution of the Laser scanner data in these situations.

Although they are preliminary, the experiments reveal that narrow roads were extracted with larger accuracy when only digital images are used, for that reason the use of the Laser scanner data is only recommended at places where there are obstructions in the lane roads.

6. References

[1] A. Baumgartner, C. Steger, H. Mayer, H. W. Eckstein, and H. Ebner, Automatic Road Extraction in Rural Areas, *Proc. International Archive Photogrammetry and Remote Sensing*, Jul. 1999, vol. 32, Part 3 (2W5), pp. 107-112.

[2] B. Solaiman, R. Fiset, and F. Cavayas, Automatic Road Extraction Using Fuzzy Mask Concepts, *Proc. International Geoscience and Remote Sensing Symposium*, IGARSS, Feb. 1999.

[3] C. Hatger, On the Use of Airborne Laser Scanning Data to Verify and Enrich Road Network Feature, *Proc. ISPRS, WG III/3, III/4, V/3 Workshop - Laser scanning*, 2005, Enschede, The Netherlands.

[4] C. R. Silva, and J. A. S. Centeno, Determination of Local Roads Widths in Images of High Resolution, *Proc. SBSR. XIV Brazilian Remote Sensing Symposium*. Natal, Brazil, Apr. 2009, pp. 7143-7149.

[5] C. R. Silva and J. A. S. Centeno. Automatic extraction of main roads using aerial images, *Pattern Recognition and Image Analysis*, v. 20, Jun. 2010, pp. 225–233.

[6] C. Wiedemann, and S. Hinz, Automatic extraction and evaluation of road networks from satellite imagery, *Proc. International Archives of Photogrammetry and Remote Sensing*, Apr. 1999, vol. 32 (3-2W5), pp. 95-100.

[7] H. Hasegawa, A Semi Automatic Road Extraction Method for Alos Satellite Imagery, *Proc. ISPRS congress*. Istanbul, Turkey, Jul. 2004, vol. 35, Part 3B; pp. 402-407.

[8] H. Liu, J. Li, and M. A. Chapman, Automated road extraction from satellite imagery using hybrid genetic algorithms and cluster analysis, *Journal of Environmental Informatics*, 2003, pp. 40-47.

[9] M. Butenuth, B. M. Straub, C. Heipke, and F. Willrich, *Tree Supported Road Extraction from Arial Images Using Global and Local Context Knowledge*, Springer-Verlag, Berlin Heidelberg, Dec. 2003, pp.162–171.

[10] N. Duta, Road Detection in Panchromatic Spot Satellite Images, *Proc. ICPR, 15th International Conference on Pattern Recognition*, Oct. 2000, vol. 4, pp. 308-311.

[11] Q. Zhang, Automated road network extraction from high spatial resolution multi-spectral imagery, *Thesis*: Doctorate in Geomatics Engineering, University of Calgary, Calgary, Jul. 2006, pp. 156.

[12] S. Clode, F. Rottensteiner, P. Kootsookos, and E. Zelniker, Detection and vectorization of roads from Lidar data, *PE&RS* (*Photogrammetric Engineering & Remote Sensing*), vol. 73, Oct. 2007, pp. 517-535.

[13] S. Clode, P. Kootsookos, and F. Rottensteiner, The Automatic Extraction of Roads from LIDAR Data, *Proc. ISPRS congress*. Istanbul, Turkey, Jul. 2004, v. 35, Part 3B; pp. 231-236.

[14] U. Bacher, and H. Mayer, Automatic Road Extraction from IRS Satellite Images in Agricultural and Desert Areas, *Proc. ISPRS congress*. Istanbul, Turkey, Jul. 2004, v. 35, Part 3B; pp. 1055-1060.

[15] Z. M. J. Valadan, and M. Mokhtarzade, Road Detection from High Resolution Satellite Images Using Artificial Neural Networks, *Proc. ISPRS congress*. Istanbul, Turkey, Jul. 2004, v. 35, Part 3B; pp. 387-392.